Virchows Arch (1999) 434:341–350

ORIGINAL ARTICLE

Tomokazu Fukuda · Toshiyuki Kobayashi
Hideaki Yasui · Masahiro Tsutsumi · Yoichi Konishi
Okio Hino

Distribution of Tsc2 protein in various normal rat tissues and renal tumours of *Tsc2* mutant (Eker) rat detected by immunohistochemistry

Received: 2 September 1998 / Accepted: 10 November 1998

Abstract Alterations in the rat tuberous sclerosis gene (*Tsc2*) are responsible for the hereditary renal carcinomas (RCs) of Eker rat. We examined protein distribution in various normal rat tissues and the Eker RCs by immunohistochemistry. Tsc2 protein is expressed in the mammary ducts, salivary glands, gastric glands, parathyroid, small and large intestine, ovary and uterus. Specific expression of Tsc2 protein is found in the B cells of pancreatic islets and in the smooth muscle of lung veins. Interestingly, in the RCs of Eker rat, Tsc2 protein was detectable with some variation in reactivity.

Key words Tsc2 protein · Renal cell carcinoma · Eker rat · Tuberous sclerosis

Introduction

The hereditary renal carcinoma (RC) of the rat originally reported by Eker in 1954 is an excellent example of a Mendelian dominantly inherited predisposition to a specific cancer in an experimental animal [1]. We and others have demonstrated that the gene responsible for Eker rat RCs is the rat homologue of the human tuberous sclerosis 2 (*TSC2*) gene [2–4]. Mutations in *TSC2* are the cause of the tuberous sclerosis complex (TSC) characterized by mental retardation and development of hamartomas in multiple organs in man [5]. Bjornsson et al. have reported that TSC-associated RCs have clinical, pathological, or genetic features distinguishing them from sporadic RCs, such as the younger age at tumour development and differences in the immunoreactivity of HMB-45 [6]. Thus, the Eker rat provides a valuable experimental model for understanding the mechanisms of disease.

In the Eker rat, one of the *Tsc2* alleles is inactivated genetically by insertion of a transposon-like sequence (inherited mutation) [3, 4]. Successive stages in the development of RCs have been observed, beginning with isolated, phenotypically altered renal tubules (which begin to appear at 2 months of age) [7], characterized by partial or total replacement of the proximal tubular epithelium by large, or weakly acidophilic cells with different degrees of nuclear atypia, or by basophilic cells (Fig. 7A). We have demonstrated the inactivation of the wild-type *Tsc2* allele in these early phenotypically altered tubules [7] and provided evidence that two hits to the *Tsc2* gene are the causative steps in renal carcinogenesis in the Eker rat, implying a tumour suppressor role [8].

The *TSC2/Tsc2* gene product contains a short region showing amino acid sequence homology to a GTPase-activating protein for Rap1 (Rap 1 GAP) [5]. Wienecke et al. reported that the human TSC2 protein has weak GAP activity for Rap1a and co-localizes with Rap1 [9]. Xiao et al. described interaction between rat Tsc2 protein and rabaptin 5, suggesting a possible association of TSC2 protein with endocytosis [10]. We earlier reported the existence of two transcriptional activation domains (AD1 and AD2) in the carboxyl terminal of the rat *Tsc2* gene product [11]. A zinc-finger-like region (our unpublished data) and a potential src-homology 3 region (SH3) binding domain are also predicted [12]. And recently, a role in the cell cycle has been indicated [13]. Although these findings point to important functions of the Tsc2 protein in vivo, the pathogenesis of Eker rat tumours and that of the human tuberous sclerosis syndrome are not fully understood. Clarification of the distribution profile of Tsc2 protein under normal and pathological conditions is a basic requirement for our understanding of this, and this has been achieved to some extent by Wienecke et al. using immunohistochemistry of human tissues affected by tuberous sclerosis (TSC) [14]. Furthermore, the organ distribution of mRNA of *Tsc2* has been assessed by in

T. Fukuda · T. Kobayashi · H. Yasui · O. Hino (✉)
Department of Experimental Pathology, Cancer Institute,
1-37-1 Kami-ikebukuro, Toshima-ku, Tokyo 170-8455, Japan
e-mail: ohino@ims.u-tokyo.ac.jp
Tel./Fax: +81-3-5394-3815

T. Fukuda · M. Tsutsumi · Y. Konishi
Department of Oncological Pathology, Cancer Center,
Nara Medical University, 840 Shijo-cho, Kashihara,
Nara 634-8521, Japan

situ hybridization in some organs of man and rodent [15, 16]. However, the localization of the TSC2/Tsc2 protein has not been reported in detail for other tissues. Furthermore, while loss of immunoreactivity to TSC2/Tsc2 antibody has been described for subependymal nodules and angiomyolipomas in human TSC or subependymal tumours in the Eker rat [17, 18], the distribution in associated RCs has received no attention. Therefore, the present study focused on the tissue distribution of Tsc2 protein and expression in RCs.

Materials and methods

A rabbit antiserum against a synthetic peptide corresponding to amino acid residues 1009–1025 of the Tsc2 protein, encoded by exon 26, was raised by repeated injection of carrier albumin-conjugated antigen with a cysteine residue at the amino terminal for coupling (CAQADDNLKNLHLELTET). This anti-peptide antibody (α-pep1) was affinity-purified by passage through EAH Sepharose 4B (Pharmacia) coupled with peptide antigen. Anti-human TSC2 carboxyl (C20) terminal peptide and its immunogen peptide were also purchased from Santa Cruz Biotech.

Male and female F344 rats (12 weeks of age) were obtained from Charles River Japan. The Eker rat was kindly provided by Dr. Knudson (Fox Chase Cancer Center, Philadelphia) and maintained by crossing with the Long Evans strain in Cancer Institute, Tokyo. Animals were anaesthetized with ether, and sacrificed. All animal experiments were performed according to the principles of laboratory animal care (NIH publication no. 85–23, revised 1985). Portions of all major organs and tissues were fixed in 10% neutral buffered formalin for 48 h and routinely processed. After embedding in paraffin, they were sectioned at 3 μm.

For Western blotting analysis, tissue protein extracts of rat various organs and COS7 cells transfected with rat *Tsc2* gene cDNA fragments [11] were extracted in sample buffer (10% glycerol, 2.3% SDS, 0.00625 M Tris-HCl pH 6.8, 5% β-mercaptoethanol) and separated by 5% (rat tissue protein) or 10% (COS7 system) polyacrylamide gel electrophoresis. The separated proteins were blotted onto IPVH nylon membranes (Millipore). After blocking with 1% skim milk in phosphate-buffered saline with 0.1% Tween 20 (PBST) overnight at 4°C, the membranes were reacted with α-pep1, C20 at 1: 200 dilution in PBST for 1 h at room temperature. They were then reacted with biotinated goat anti-rabbit IgG at 1:500 dilution for 1 h at room temperature. Signals were detected with the ECL western blotting detection system (Amersham).

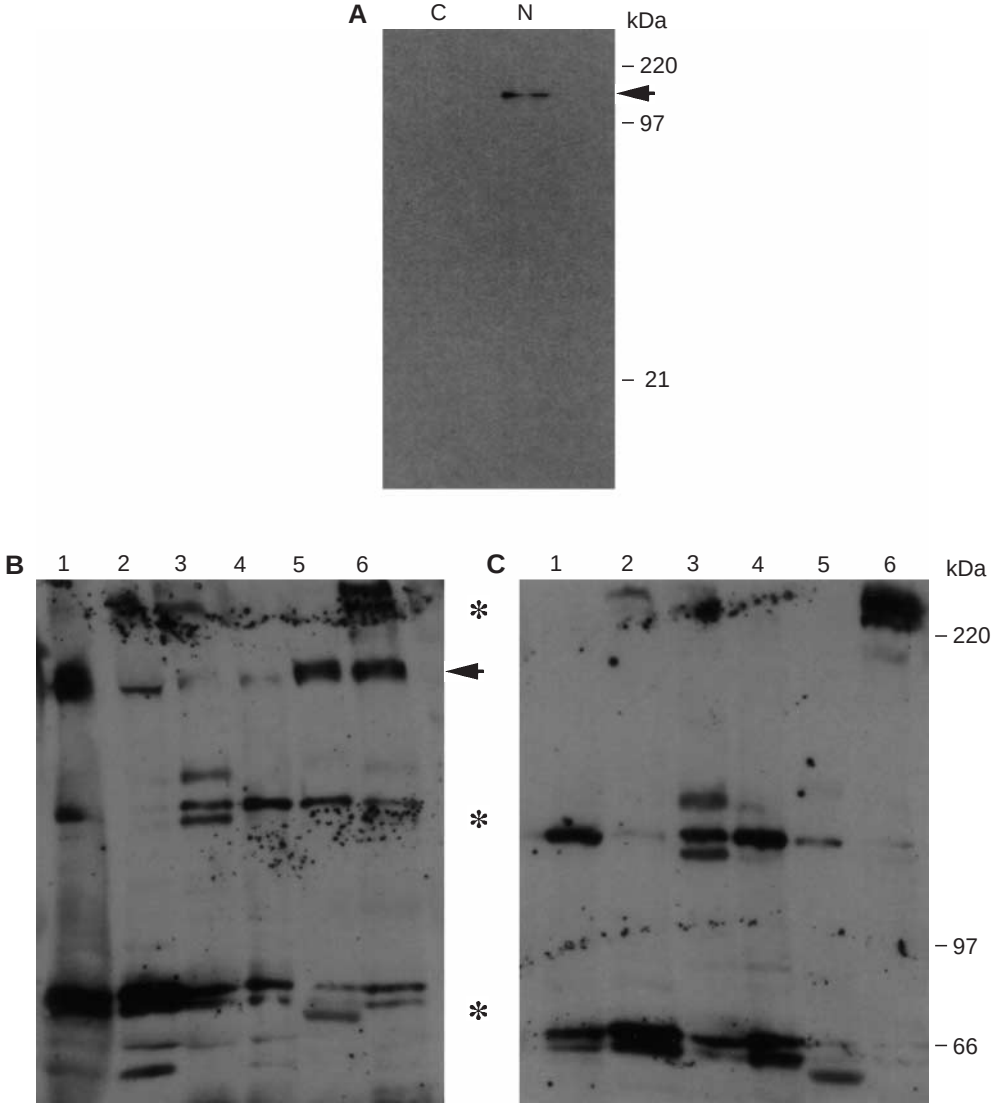

Fig. 1A–C Results of western blot analysis using anti-Tsc2 antibodies. **A** Western blot analysis with α-pep1 of proteins from COS7 cell expressing rat Tsc2 with (*lane N*) or without (*lane C*) the pep1 amino acid sequence. The *arrow* indicates the Tsc2 band of the predicted size (110 kDa). **B** Western blot analysis with C20 of tissue proteins from brain (*lane 1*), heart (*lane 2*), mammary gland (*lane 3*), kidney (*lane 4*), spinal cord (*lane 5*) and ovary (*lane 6*). The *arrow* indicates Tsc2 bands of the predicted size (180 kDa). **C** Western blot analysis by preabsorbed C20 antibody. Signals of Tsc2 generated in panel B in 180 kDa were absorbed. Nonspecific signals are indicated by the *asterisks*. *Lanes* as in **B**

For immunostaining, tissue sections were deparaffinized, preheated in 10 mM citrate buffer (pH 6.0) in a microwave oven, and pretreated with 3% H_2O_2 solution for 20 min. Blocking was performed using 10% normal goat serum (NGS) /Tris-buffered saline (TBS). Then, sections were incubated with α-pep1 or C20 (1/200–500 dilution in 10% NGS/TBS) overnight at 4°C or room temperature respectively, and then with a 1: 300 dilution of biotinated goat anti-rabbit IgG (Dako) in TBS for 1.5 h for pep1 or overnight for C20. Sections were subsequently incubated with avidin and biotin–peroxidase complex (DAKO). Binding was demonstrated using 3,3'-diaminobenzidine tetrahydrochloride (DAB, Sigma) and H_2O_2 (0.03%) as the substrates, followed by counterstaining with haematoxylin. For controls, sections were incubated with primary antibodies preabsorbed with the relevant specific peptides.

For identification of positive cell type in pancreatic islets, double immunostaining was performed. After detection using α-pep1 as described above, sections of pancreas were incubated either with a guinea pig polyclonal antibody against human insulin (Dako), or a rabbit polyclonal antibody against human somatostatin (Novocastra), or a rabbit polyclonal antibody against human glucagon (Novocastra) for 1 h in room temperature. All of these antibodies were diluted in 10% NGS/TBS at 1: 200. After primary antibody reaction, fluorescein-iso-thiocyanate (FITC)-conjugated rabbit anti-guinea pig or tetraethylrhodamine-isithio-cyanate (TRITC)-conjugated swine anti-rabbit IgG (Dako) at 1:200 diluted in 10% NGS/TBS was reacted for 1 h at room temperature. Sections were counterstained with haematoxylin. Samples were examined under a phase-contrast fluorescence microscope (Nikon).

Results

Initially, we performed western blot analysis to assess the specificity of α-pep1 C20 antibodies. α-pep1 did not work well for rat tissues or cell extracts, probably due to the low titre. However, a clear band of the predicted size (about 110 kDa) was detected in extracts of COS7 cells transiently transfected with plasmids expressing the amino terminal portion of the rat Tsc2 protein (Fig. 1A). This band was not found with COS7 cells transiently expressing the carboxyl terminal half of the Tsc2 protein (Fig. 1A). We also tested the cross-reactivity of commercially obtained C20 antibody, which recognizes the carboxyl terminal 20 amino acid sequence of the human TSC2 protein. The peptide sequence of the carboxyl terminal of rat Tsc2 protein differs by three amino acids within this 20-amino acid stretch. However, a band of rat Tsc2 protein at 180 kDa was detected in several tissue extracts, and COS7 cells bearing a full-length rat Tsc2 cDNA were deleted by Western blot analysis using C20 (Fig. 1B, and data not shown). We confirmed that the band detected was absorbed when the primary antibody was pretreated with specific peptide (Fig. 1C). Immunohistochemical staining demonstrated that most tissues displayed common reactions for both α-pep1 and C20 (representative result is shown in Fig. 2A, B). Most immunoreactivity disappeared when the anti-peptide antibodies were pretreated with each of the immunogenic peptides (Fig. 2C, D).

Immunohistochemical analysis was performed using α-pep1 and C20 for abdominal skin, adrenal glands, brain, epididymis, eyeballs, harderian glands, heart, kidney, large and small intestine, liver, lung, lymph nodes

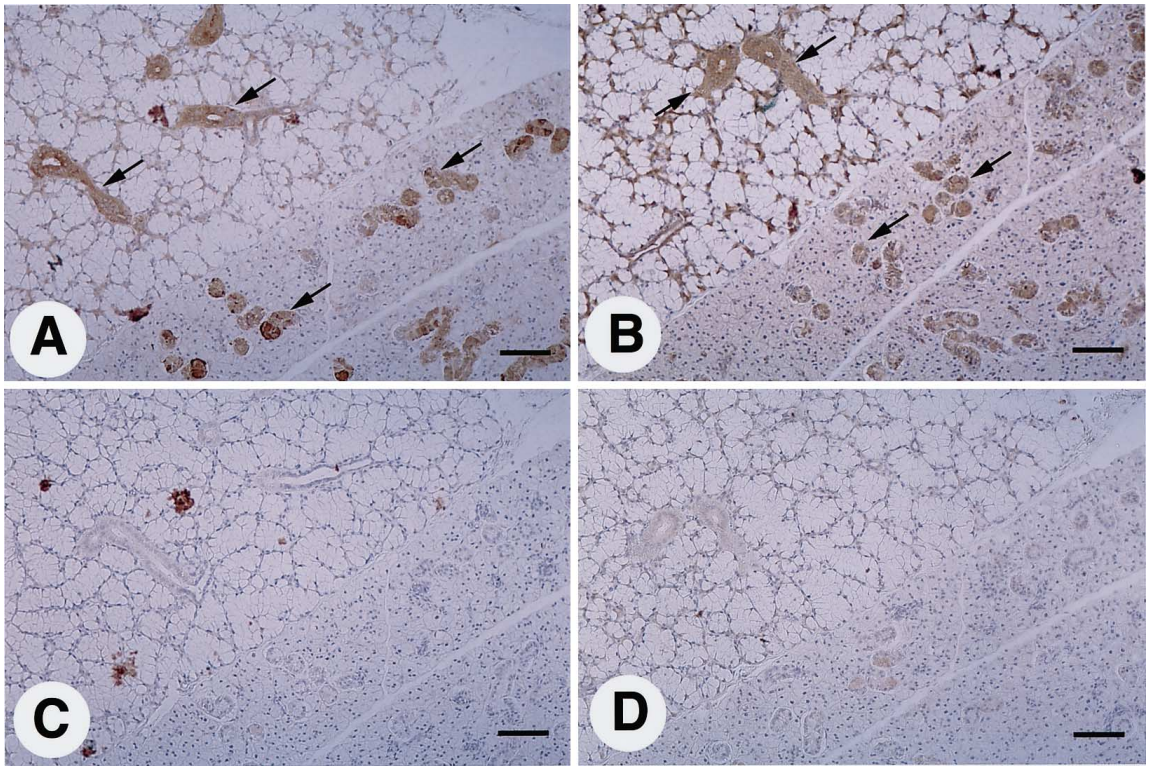

Fig. 2A–D Immunostaining of Tsc2 in salivary gland with α-pep1 and C20, and their absorbed antibodies. **A** The interlobular and excretory ducts are positively stained in salivary glands by α-pep1 (*arrow*). **B** The interlobular and extrary ducts are similarly stained with C20 (*arrow*). **C, D** Immunostaining with preabsorbed α-pep1 and C20 antibodies. Reduced staining is observed compared with **A** and **B**. In all cases counterstaining was performed with haematoxylin. *Scale bar* 100 μm

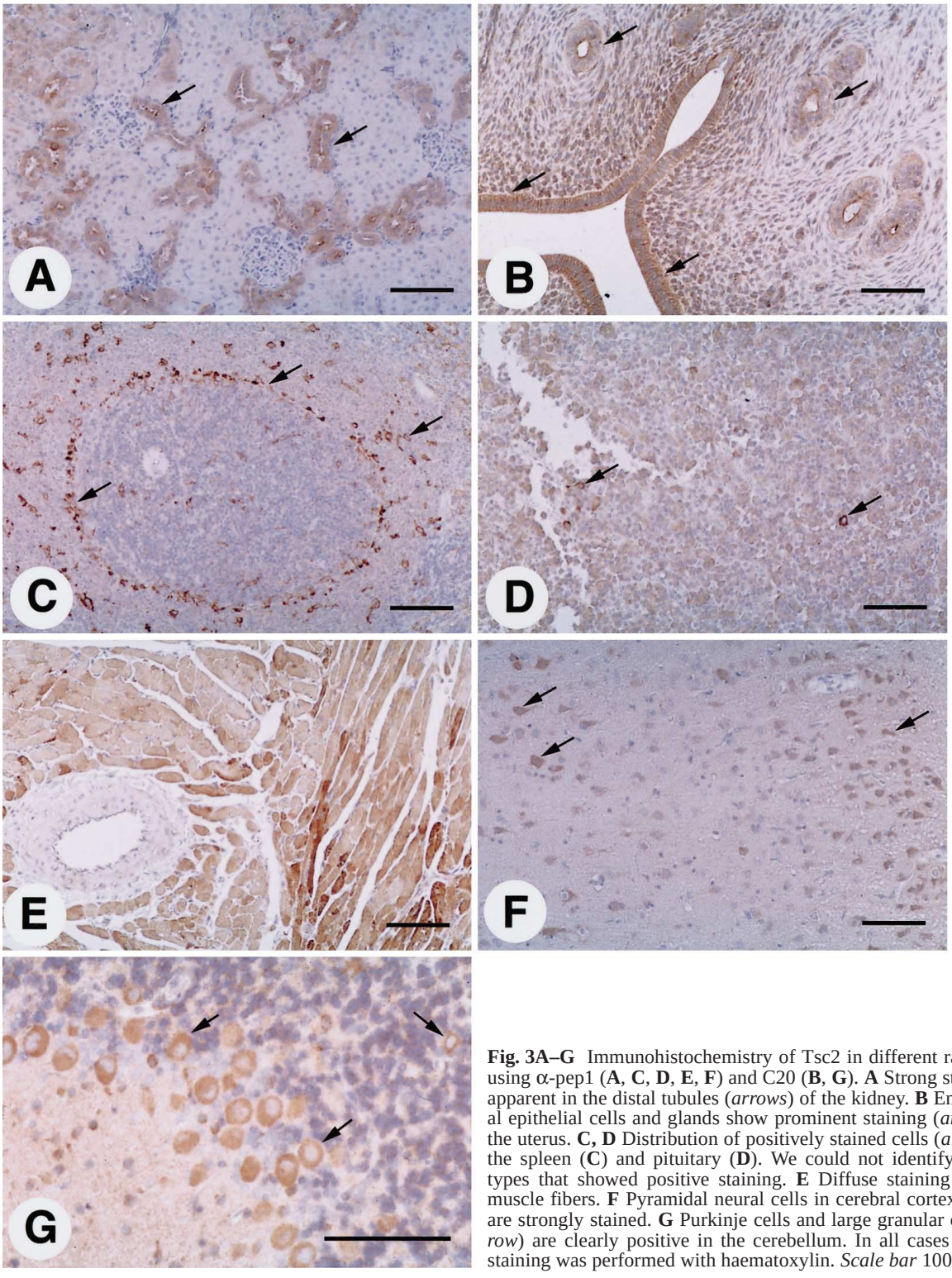

Fig. 3A–G Immunohistochemistry of Tsc2 in different rat organs using α-pep1 (**A**, **C**, **D**, **E**, **F**) and C20 (**B**, **G**). **A** Strong staining is apparent in the distal tubules (*arrows*) of the kidney. **B** Endometrial epithelial cells and glands show prominent staining (*arrows*) in the uterus. **C, D** Distribution of positively stained cells (*arrows*) in the spleen (**C**) and pituitary (**D**). We could not identify the cell types that showed positive staining. **E** Diffuse staining of heart muscle fibers. **F** Pyramidal neural cells in cerebral cortex (*arrow*) are strongly stained. **G** Purkinje cells and large granular cells (*arrow*) are clearly positive in the cerebellum. In all cases counterstaining was performed with haematoxylin. *Scale bar* 100 µm

(mandibular), pancreas, parathyroid, pituitary gland, skeletal muscle, spleen, stomach, tongue and urinary bladder. The ovary and uterus in females, and the prostate, seminal vesicles and testis in male rats were also examined. Anti-Tsc2 antibodies revealed positive staining in various epithelial tissues, the nervous system and muscle fibres. Positive signals were cytoplasmically localized in all tissues examined, with very little binding in the nuclei, as confirmed by microscopic examination before counterstaining. There were no differences between male and female rats in immunoreactivity for the same tissues.

We previously reported that all Eker heterozygous mutants developed renal RCs about 1 year after birth

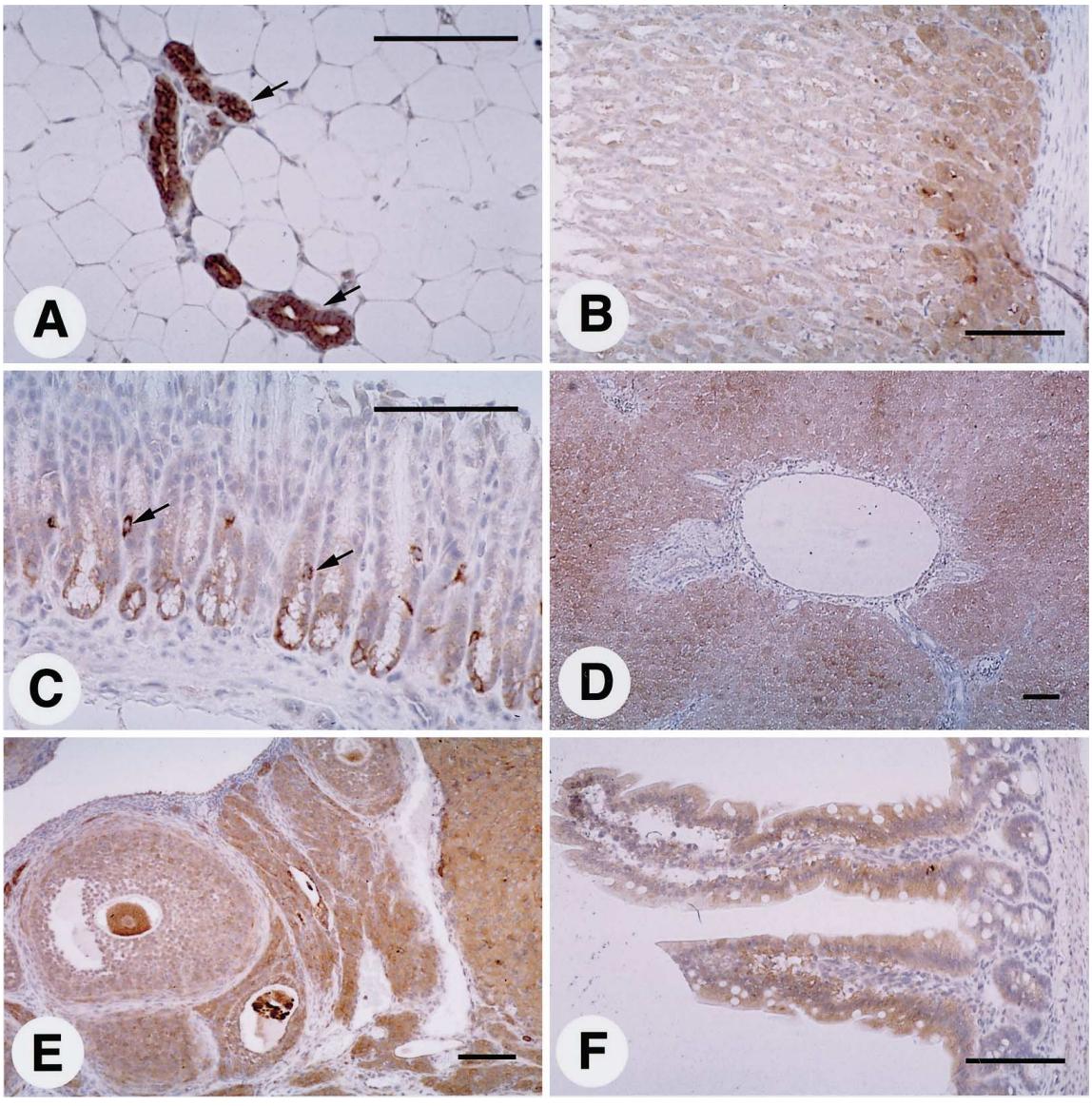

Fig. 4A–F Immunohistochemistry of Tsc2 in organs in which abnormalities have rarely reported in human TSC patients or the Eker rat. All panels staining with α-pep1. **A** Ductal epithelial cells of mammary ducts are strongly stained (*arrow*). **B** Diffuse immunoreactivity is apparent in fundic glands. **C** Parietal cells are prominently stained in the pyloric glands (*arrow*). **D** Tsc2 protein is diffusely distributed in the liver parenchyma but is negative in the central veins and bile ducts. **E** Immunostaining of Tsc2 protein in an ovary. **F** Surface absorptive epithelial cells and intestinal glands show immunoreactivity in the small intestine. *Scale bar* 100 μm

[19]. In addition, leiomyomas/ leiomyosarcomas of the uterus and pituitary adenomas and haemangiomas/haemangiosarcomas of the spleen are often encountered [20–22]. First of all, we examined the distribution of Tsc2 protein in these organs in normal rats. Diffuse staining was observed in renal tubules throughout the cortex of the normal kidney. Distal tubules were strongly and proximal tubules, faintly stained (Fig. 3A). In the medulla of the kidney, solid staining of the collecting tubules was observed (data not shown). No staining was detected in the renal blood vessels and glomeruli in this study, whereas small blood vessels in kidney and many other organs were reported to be immunoreactive with anti-Tsc2 antibodies in man [14]. In the uterus, prominent staining of the endometrial epithelial cells and glands was detected (Fig. 3B). Although the smooth muscle in the uterus was also reactive, the intensity was fainter than for epithelial cells. In the spleen, dominant staining was noted in the germinal centres and scattered staining in the mantle zone, but none in the central or trabecular arteries (Fig. 3C). In the pituitary, some cells showed solid staining in a diffuse background. We could not identify the cell types that showed immunoreactivity in the spleen and pituitary (Fig. 3D).

Human patients affected by TSC often develop rhabdomyomas of the heart, angiomyolipomas of the kidney, cortical tubers and subependymal nodules of the brain with highly variable phenotypes [23]. Therefore, we also examined the distribution of Tsc2 protein in the

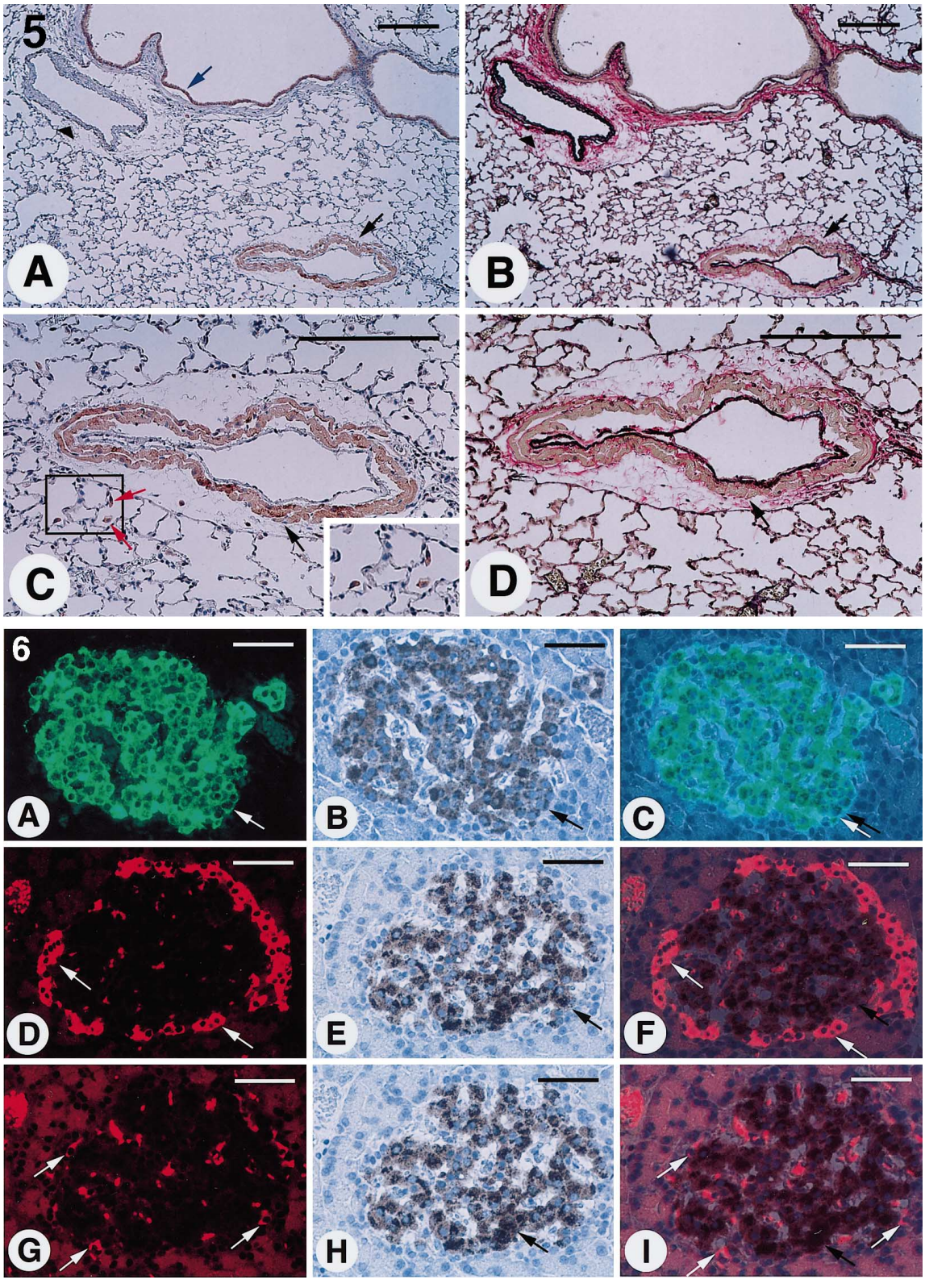

Fig. 5A–D Immunostaining of Tsc2 protein with α-pep1 and Elastica van Gieson staining (EVG) in rat lung. Serial sections were used for comparison. **A, C** Staining features of Tsc2 protein in rat lung. The immunoreactive vessel (*black arrows*) is further from the bronchus than the nonreactive one (**A** *arrowhead*). Bronchial epithelial cells (**A** *blue arrow*) and alveolar macrophages (**C** *red arrow*) display reactivity. The staining feature of alveolar macrophage is shown at a higher magnification in the *right lower column* in **C**. **B, D** EVG staining in rat lung. The vein, containing elastic fibres only in the inner layer is indicated by the *black arrow* (**B**). The artery containing them throughout the vessel wall is indicated by the *arrowhead* (**B**). *Scale bar* 100 µm

Table 1 Summary of immunoreactive organs and tissues in rats

Organs	Tissues and cells demonstrating positive staining with Tsc2 antibodies
Adrenals	Strongly positive cells within areas of diffuse staining in the medulla[a]
Brain (cerebral cortex)	Dominant staining in pyramidal neural cells in diffuse backgrounds
Brain (cerebellum)	Purkinje cells and large granular cells
Kidney	Faint staining in proximal tubules and strong staining in distal or collecting tubules
Heart	Muscle fibres
Lung	Bronchial epithelium, alveolar macrophages, smooth muscle of vein
Liver	Hepatocytes (no staining of bile ducts or blood vessels)
Mammary glands	Ductal epithelial cells of mammary ducts
Mandibular lymph node	Postcapillary venules of the marginal sinus
Ovary	Oocytes, follicular epithelial cells of stratum granulosum, ovarian cumulus, theca interna and corpus luteum
Pancreas	B cells in pancreatic islets
Parathyroid	Chromophobic cells
Pituitary	Some cells showed solid staining in diffuse backgrounds[a]
Retina	Rods and cones, inner granular layer, layer of nerve fibres and ganglion cells
Salivary glands	Interlobular and excretory ducts
Seminal epididymis	Epithelial cells in the ducts of epididymis and seminal ducts
Skeletal muscle	Muscle fibres
Small and large intestine	Surface absorptive epithelial cells, goblet cells and intestinal glands
Spleen	Scattered stained cell in the germinal centre and mantle zone[a]
Stomach	Diffuse staining in gastric proper glands and prominant staining in enterochromaffin cells
Testis	All spermatocytes regardless of the stage of spermatogenesis
Tongue, abdominal skin	Muscle fibres
Uterus	Endometrial epithelial cells and glands, muscle fibres

[a] The immunoreactive cells could not be identified in this study

heart and brain of rats. In the heart, diffuse staining of all muscle fibres could be detected (Fig. 3E). High expression of *Tsc2* mRNA in heart has also been found previously by northern blotting [4]. Tsc2 antibodies showed reactivity in pyramidal neural cells in the cerebral cortex, and also in glial cells of white matter to a lesser extent (Fig. 3F). We could not observe any positive staining in neural nuclei; nucleus ruber, substantia nigra and nucleus nervi oculomotrii were all negative (data not shown). In the cerebellum, prominent staining of Purkinje cells and of large granular cells in the granular cell layer (Fig. 2G) was detected. Small granule cells displayed a perinuclear staining pattern. This distribution of Tsc2 protein in the brain was similar to that detected earlier by immunohistochemistry [14] or in situ hybridization for human TSC2 expression [24].

Ductal epithelial cells of mammary glands were found to be strongly positive (Fig. 4A), even in subcutaneous fat where mammary glands were not mature, in 12 week-old female rats. The existence of Tsc2 protein in mammary tissue was confirmed by western blotting analysis with C20 antibody (Fig. 1B). Intense staining was observed in the interlobular and excretory ducts of the salivary gland (Fig. 2A, B). In the gastric glands proper, there was diffuse immunoreactivity in the fundic glands (Fig. 4B), with more prominent staining of the parietal cells and enterochromaffin cells (EC cell) of the pyloric glands in the stomach (Fig. 4C).

In the lung, bronchial epithelium and alveolar macrophages showed positive staining (Fig. 5A, C). In addition, some, but not all, blood vessels showed immunoreactivity (Fig. 5A). Those more distant from the bronchus demonstrated stronger staining. Elastica van Gieson (EVG) staining of serial sections (Fig. 5B, D) demonstrated that blood vessels containing elastic fibres only in the inner layer were immunoreactive, while these with elastic fibers throughout their walls were not. Thus, veins, and but not arteries, appeared to be immunoreactive. Furthermore, the immunoreactive tissue in the lung vein was seen to stain yellow ochre in EVG staining (Fig. 5D). From the staining features of the EVG section and the morphology in haematoxylin and eosin-stained section (data not shown), we suspected the immunoreactive tissue in lung vein might be the smooth muscle.

In the pancreas, prominent staining of pancreatic islets was detected (Fig. 6 B, E, H). Double immunostaining for insulin, glucagon or somatostatin allowed identification of the type of positive cells (Fig. 6). Almost all immunoreactive cells with α-pep1 were also reactive with the insulin antibody (Fig. 6A and C). In contrast, cells that were immunoreactive against somatostatin or glucagon antibodies showed no reactivity with α-pep1 (Fig. 6 D–I). We conclude that the B cells of pancreatic islet express the Tsc2 protein in rats.

Table 1 summarizes the results for Tsc2 distribution in organs and tissues that showed immunoreactivity. Immunostaining features of the ovary, liver and small intestine are also illustrated in Fig. 4D–F.

◀ **Fig. 6A–I** Identification of Tsc2-immunoreactive cells in pancreatic islet. **A, D, G** Fluorescent immunostaining of insulin (**A**), glucagon (**D**) and somatostatin (**G**). *White arrows* indicate immunoreactive cells. **B, E, H** Immunostaining using α-pep1. *Black arrows* indicate α-pep1-immunoreactive cells. **C, F, I** Double immunostaining for α-pep1 and insulin (**C**), glucagon (**F**) and somatostatin (**I**). There is good agreement only in the case of insulin **C**. *Scale bar* 50 μm

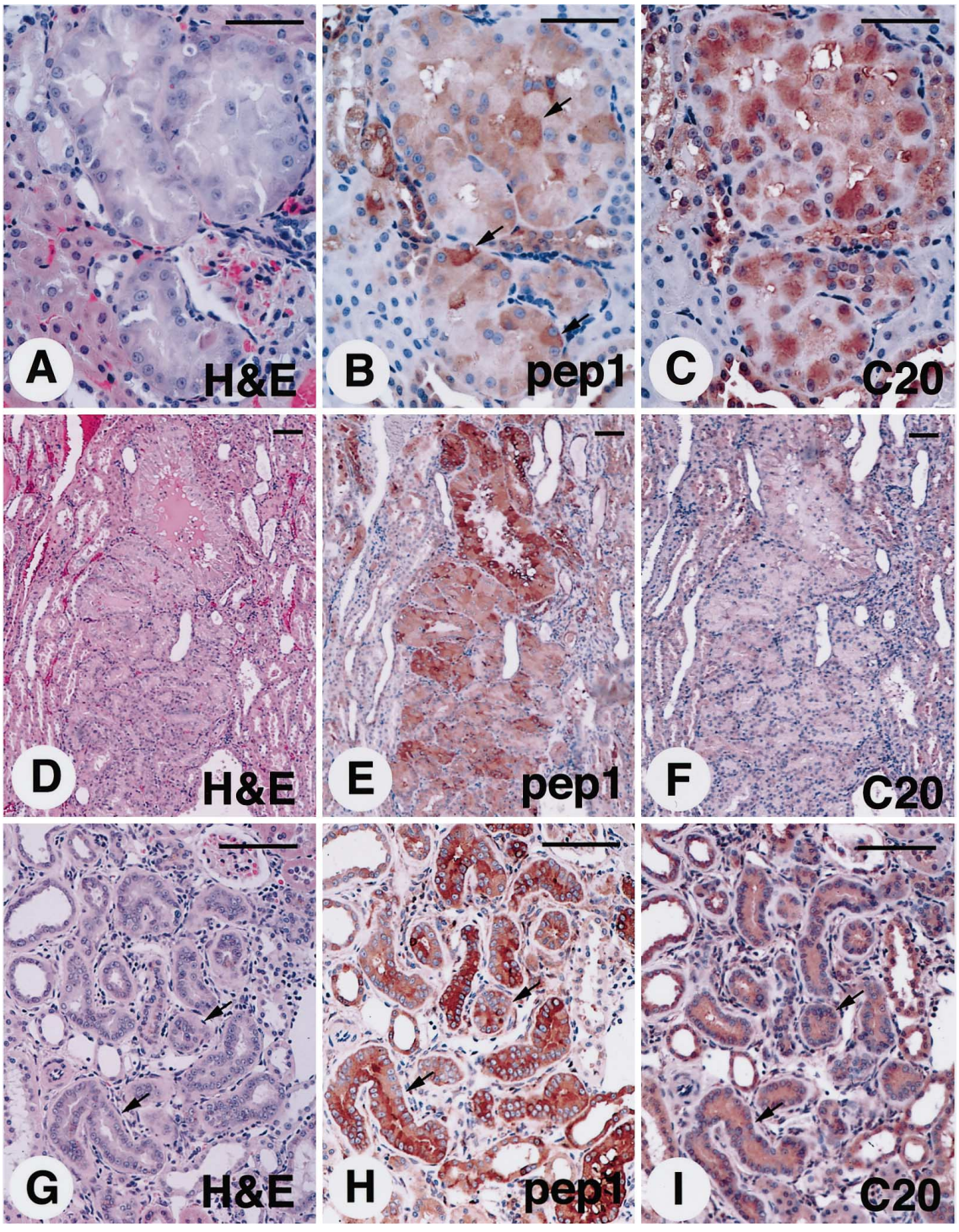

Fig. 7 Immunostaining of Tsc2 protein in regenerative tubules and tumors in Eker rats. Serial sections were used to allow exact comparison. **A, B, C** Immunostaining pattern and morphology of a Eker altered tubule showing immunoreactivity with both antibodies. **D, E, F** Immunostaining and morphology of a Eker renal tumor showing different reaction patterns with α-pep1 (E) and C20 (F). **G, H, I** Spontaneously developing regenerative tubules (*arrow*) in an Eker rat with spontaneous chronic nephritis. *Scale bar* 100 µm

Results for immunoreactivity of spontaneous RCs and preneoplastic tissues in Eker rats using α-pep1 and C20 antibodies in serial sections are illustrated in Fig. 7. Scattered staining of some RC cells was observed with α-pep1, this being strong in some cases (Fig. 7B; *black arrow*). Most phenotypically altered tubules demonstrated reactivity with both antibodies. However, some RCs reacted with α-pep1 but not C20 (Fig. 7 E, F). Two histopathological types of RCs, compact and tubular, can be distinguished in Eker rats, on haematoxylin-eosin stain-

ing. However, there was no apparent relation between the histological type and the Tsc2 staining pattern.

In rats with spontaneous chronic nephritis, regenerative tubules are often observed. Such regenerative tubules were highly immunoreactive to Tsc2 antibodies (Fig. 7G–I).

Discussion

The present study, using two independently prepared antibodies, α-pep1 and C20, demonstrated the existence of Tsc2 protein in various organs and tissues in which abnormalities have rarely been observed in human TSC or the Eker rat. In kidney, higher expression of Tsc2 protein was detected in distal tubules than in proximal tubules. We suspect that most RCs in the Eker rat originate from proximal tubules [19]. Therefore, we concluded that the organs and tissues that express Tsc2 protein strongly are not at high risk of tumour development in man or the Eker rat. However, there is a possibility that cells change their production of Tsc2 protein depending on the circumstances. Thus, we detected strong expression in regenerative tubules in animals after spontaneous nephritis (Fig. 7G–I).

In contrast to Wienecke et al. who reported intense staining of small blood vessels in many organs, including the kidney, skin, and adrenal glands in man [14], we could not detect any staining of small blood vessels in the kidney or adrenal glands in the rat. They proposed that loss of function of TSC2 protein in small blood vessels might be a cause of highly vascular tumours in human TSC patients. Although this difference in immunoreactivity of small blood vessels might be due to species specificity, we also failed detect TSC2 protein in small blood vessels of human kidney, salivary glands, brain, adrenal glands and pancreas with the two antibodies used in the present study (Yasui et al. manuscript in preparation). Since the C20 antibody was also applied by Wienecke et al. additional studies are needed to clarify this anomaly.

We have demonstrated that B cells in rat pancreatic islets express Tsc2 protein. Recently Kim et al. reported that human TSC patients occasionally develop insulinomas [25]. Whether loss of function of Tsc2 protein in B cells might be causally involved deserves consideration.

In addition to the pancreatic islets, veins, but not arteries, showed staining in rat lung. The staining was also observed in postcapillary venules in lymph nodes. Although pathological abnormalities of Eker rat lung and lymph node have not been reported, human TSC patients are reported to develop the lymphangiomyomatosis (LAM) that consists of proliferated immature smooth muscle in lung tissue and proliferation of endothelial cell at lymphatic wall in lymph nodes [26]. The distribution of Tsc2 protein in rat lung and lymph node should be noted in consideration of the pathogenesis of LAM in human TSC patients.

In fact, Tsc2 protein was detected in many exocrine and endocrine organs. Although we still do not know the real function of TSC2/Tsc2 protein in vivo, the distribution found suggests a possible role in protein production for export. In a previous study in vitro, localization of TSC2 protein in Golgi apparatus was found by Wienecke et al. (1997) [9]. In another report, an association with rabaptin-5 that binds to the active form of Rab5 GTPase was reported [10]. Rab5 GTPase is a critical component of the docking and fusion process of the endocytic pathway. Since exocrine and endocrine cells contain well-developed Golgi apparatuses, a role of Tsc2 protein in secretory vesicle formation is conceivable. However, in view of the existence of various secretory tissues that do not express Tsc2 protein, such as prostate and acinous tissue of pancreas, its contribution must be specific rather than general in nature.

Loss of TSC2 protein in cortical tubers and angiomyolipomas has been observed in human TSC patients [17, 27]. In addition, loss of Tsc2 protein in Eker rat subependymal hamartomas appears typical [18]. However, Eker rat RCs showed reactivity to Tsc2 antibodies on immunohistochemistry, and a similar situation clearly does not exist for renal carcinogenesis. Thus, loss of immunoreactivity is not necessary for renal carcinogenesis in the Eker rat. However, the lack of complete consistency of results with the two antibodies might suggest an alteration in the protein. Differences in inactivation (2nd hit) of the wild-type *Tsc2* allele would explain our results [28]. Deletion of the wild-type allele would be expected to cause loss of immunoreactivity, but missense mutations that cause amino acid substitutions would have more subtle effects, and some have no influence on immunoreactivity. We earlier demonstrated that the Eker insertion creates abnormal *Tsc2* mRNAs and a premature translational termination lacking the carboxyl-terminal portion of the product [3, 29]. Although the existence of truncated Tsc2 protein could not been confirmed by western blot analysis owing to the scarcity of samples, if such proteins lacking the carboxyl-terminal portion of Tsc2 protein actually exist, this might be why some RCs are immunoreactive to α-pep1, but not to C20.

Clarification of the exact reasons for variation in Tsc2 immunoreactivity in the Eker rat RCs may provide clues to their pathogenesis.

Acknowledgements This work was supported in part by a Grant-in-Aid for Cancer Research from the Ministry of Education, Science, Sports and Culture of Japan and the Organization for Pharmaceutical Safety and Research (OPSR). We thank Dr. K. Nishida (Saitama Cancer center, Japan) and Dr. M. Yoshida (Sasaki Institute, Japan) for special advice for histopathological judgment. We thank Ms. K. Nomura (Cancer Institute, Department of Pathology) for technical advice regarding immunostaining. We also thank Drs. H Sugano, T. Kitagawa and A.G. Knudson for their encouragement throughout this work.

References

1. Eker R, Mossige J (1961) A dominant gene for renal adenomas in the rat. Nature 189:858–859
2. Hino O, Kobayashi T, Tsuchiya H, Kikuchi Y, Kobayashi E, Mitani H, Hirayama Y (1994) The predisposing gene of the

Eker rat inherited cancer syndrome is tightly linked to the tuberous sclerosis (*TSC2*) gene. Biochem Biophys Res Commun 203:1302–1308
3. Kobayashi T, Hirayama Y, Kobayashi E, Kubo Y, Hino O (1995) A germline insertion in the tuberous sclerosis (*Tsc2*) gene gives rise to the Eker rat model of dominantly inherited cancer. Nat Genet 9:70–75
4. Yeung R, Xiao G, Jin F, Lee W, Testa J, Knudson A (1994) Predisposition to renal carcinoma in the Eker rat is determined by germ-line mutation of the tuberous sclerosis 2 (*TSC2*) gene. Proc Natl Acad Sci USA 91:11413–11416
5. European Chromosome 16 Tuberous Sclerosis Consortium (1993) Identification and characterization of tuberous sclerosis gene on chromosome 16. Cell 75:1305–1315
6. Bjornsson J, Short MP, Kwiatkowski DJ, Henske EP (1996) Tuberous sclerosis-associated renal cell carcinoma. Am J Pathol 149:1201–1208
7. Kubo Y, Klimek F, Kikuchi Y, Bannasch P, Hino O (1995) Early detection of Knudson's two-hits in preneoplastic renal cells of the Eker rat model by laser microdissection procedure. Cancer Res 55:989–990
8. Orimoto K, Tsuchiya H, Kobayashi T, Matsuda T, Hino O (1996) Suppression of the neoplastic phenotype by replacement of the *Tsc2* gene in Eker rat renal carcinoma cells. Biochem Biophys Res Commun 219:70–75
9. Wienecke R Jr, Shoarinejad F, Vass WC, Reed J, Bonifacino JS, Resau JH, Gunzburg JD, Yeung RS, DeClue JE (1997) Colocalization of Tsc2 product tuberin with its target Rap1 in the Golgi apparatus. Oncogene 13:913–923
10. Xiao G-H, Shoarinejad F, Jin F, Golemis EA, Yeung RS (1997) The tuberous sclerosis 2 gene product, tuberin, functions as a Rab5 GTPase activating protein (GAP) in modulating endocytosis. J Biol Chem 272:6097–6100
11. Tsuchiya H, Orimoto K, Kobayashi T, Hino O (1996) Presence of potent transcriptional activation domains in the predisposing tuberous sclerosis (*Tsc2*) gene product of the Eker rat model. Cancer Res 56:429–433
12. Olsson PG, Schofield JN, Edwards YH, Frischauf AM (1996) Expression and differential splicing of the mouse TSC2 homolog. Mamm Genome 7:212–215
13. Soucek T, Pusch O, Wienecke R, DeClue JE, Hengstschlager M (1997) Role of the tuberous sclerosis gene-2 product in cell cycle control. J Biol Chem 272:29301–29308
14. Wienecke R Jr, Reed JA, Gunzburg JD, Yeung RS, DeClue JE (1997) Expression of Tsc2 product tuberin and its target Rap1 in normal human tissue. Am J Pathol 150:43–50
15. Menchine M, Emein JK, Mischel PS, Haag TA, Norman MG, Pepkowitz SH, Welsh CT, Townsend JJ, Vinters HV (1996) Tissue and cell-type specific expression of the tuberous sclerosis gene, Tsc2, in human tissues. Mod Pathol 9:1071–1080
16. Xiao GH, Jin F, Yeung RS (1995) Identification of tuberous sclerosis 2 messenger RNA splice variants that are conserved and differentially expressed in rat and human tissues. Cell Growth Differ 6:1185–1191
17. Mizuguchi M, Kato M, Yamanouchi H, Ikeda K, Takashima S (1996) Loss of tuberin from cerebral tissues with tuberous sclerosis and astrocytoma. Ann Neurol 40:941–944
18. Henske EP, Wessner LL, Golden J, Scheithauer BW, Vortmeyer AO, Zhuang Z, Klein-Szanto AJP, Kwiatkowski DJ, Yeung RS (1997) Loss of tuberin in both subependymal giant cell astrocytomas and angiomyolipomas supports a two-hit model for the pathogenesis of tuberous sclerosis tumors. Am J Pathol 151:1639–1647
19. Hino O, Klein-Szanto AJP, Freed JJ, Testa JR, Brown DQ, Vilensky M, Yeung RS, Tartof KD, Knudson AG (1993) Spontaneous and radiation-induced renal tumors in the Eker rat model of dominantly inherited cancer. Proc Natl Acad Sci USA 90:327–331
20. Hino O, Mitani H, Katsuyama H, Kubo Y (1994) A novel cancer predisposition syndrome in the Eker rat model. Cancer Lett 83:117–121
21. Kubo Y, Kikuchi Y, Mitani H, Kobayashi E, Kobayashi T, Hino O (1995) Allelic loss at the tuberous sclerosis (*Tsc2*) gene locus in spontaneous uterine leiomyosarcomas and pituitary adenomas in the Eker rat model. Jpn J Cancer Res 86:828–832
22. Kubo Y, Mitani H, Hino O (1994) Allelic loss at the predisposing gene locus in spontaneous and chemically induced renal cell carcinomas in the Eker rat. Cancer Res 54:2633–2635
23. Geist RT, Gutmann DH (1995) The tuberous sclerosis 2 gene is expressed at high levels in the cerebellum and developing spinal cord. Cell Growth Differ 6:1477–1483
24. Kerfoot C, Wienecke R, Menchine M, Emein J, John C. Maize J, Welsh CT, Norman MG, DeClue JE, Vinters HV (1996) Localization of tuberous sclerosis 2 mRNA and its protein product tuberin in normal human brain and in cerebral lesions of patients with tuberous sclerosis. Brain Pathol 6:367–377
25. Kim H, Kerr A, Morehouse H (1995) The association between tuberous sclerosis and insulinoma. Am J Neuroradiol 16:1543–1544
26. Lie JT (1988) Pulmonary manifestations. In: Gomez MR (ed) Tuberous sclerosis. Raven, New York, pp 159–167
27. Kimura N, Watanabe M, Date F, Kitamoto T, Kimura I, Horii A, Nagura H (1997) HMB-45 and tuberin in hamartomas associated with tuberous sclerosis. Mod Pathol 10:952–959
28. Kobayashi T, Urakami S, Hirayama Y, Yamamoto T, Nishizawa M, Takahara T, Kubo Y, Hino O (1997) Intragenic Tsc2 somatic mutations as Knudson's second hit in spontaneous and chemically induced renal carcinomas in Eker rat model. Jpn J Cancer Res 88:254–261
29. Kobayashi T, Nishizawa M, Hirayama Y, Kobayashi E, Hino O (1995) cDNA structure, alternative splicing and exon-intron organization of the predisposing tuberous sclerosis (*Tsc2*) gene of the Eker rat model. Nucleic Acids Res 23:2608–2613